MULTI-COLOR PYROMETER FOR MATERIALS PROCESSING IN SPACE

Michael B. Frish
Mark N. Spencer
Nancy E. Wolk
Jennifer S. Werner

Physical Sciences Inc.
Research Park, P.O. Box 3100
Andover, MA 01810

and

Henry A. Miranda Jr.
Miranda Laboratories
1 De Angelo Drive
Bedford, MA 01730

1. INTRODUCTION

This paper describes the design, construction, and calibration of a computer-linked multicolor pyrometer which can be used for accurately measuring the temperatures (between 300 and 2000 C, ±2.5 percent) of materials having emissivities known to only within ±25 percent. In addition, the device was constructed in a manner which demonstrates that it can be readily adapted to a spacecraft and used to control or regulate thermal processes for manufacturing materials in space.

The work is described in five sections. Section 2 presents background information including the theory underlying our pyrometer design. Section 3 describes the design in detail and justifies the selection of components. Section 4 discusses the procedure used to calibrate and test the resulting device, while a demonstration of its accuracy when measuring temperatures of surfaces having somewhat unknown emissivities is presented in Section 5. Section 6 shows how the device has been coupled to a computer and used as a non-contact temperature controller. A summary of the work comprises Section 7.

2. BACKGROUND

New techniques for processing of materials in space are presently being investigated by NASA and by others interested in expanding the frontiers of commercial materials manufacturing. As with any manufacturing process, it is essential that certain properties which vary during the processing, or which enable control of the process, be measured accurately. Commercial devices which are spaceworthy and capable of accurate, non-contact measurements with capablilties for incorporation into automated systems are quite inadequate. To help fill this void, we have developed an optical pyrometer, employing state-of-the-art optronics and computational techniques, capable of accurately measuring sample temperatures within the temperature range of 300 to 2000 C.

Pyrometry is a well-established technique for deducing the approximate temperature of a heated object by measuring the radiant energy which it emits. The radiant emission is determined by the Planck equation[1]

$$R(\lambda)d\lambda = C_1/(\pi\lambda^5)\ \left[\varepsilon(\lambda,T)/\left\{\exp(C_2/\lambda T)-1\right\}\right]d\lambda \qquad (1)$$

where $R(\lambda)d\lambda$ is the radiant flux per steradian per unit area of emitter surface in the wavelength interval $[\lambda,\ \lambda + d\lambda]$, $C_1/\pi = 1.191 \times 10^{-12}$ W-cm^2/sr, $C_2 = 1.44$ cm-K, T is the temperature, and $\varepsilon(\lambda,T)$ is the spectral emissivity of the material at wavelength λ. In a typical pyrometer system, a portion of the heated target's surface is imaged by a lens or concave mirror onto a photodetector which converts the incident radiation into an measurable quantity. For measurement of temperatures over small, isothermal regions, a photodiode or photomultiplier is a commonly used transducer. The optical path generally contains several windows, mirrors, beam splitters or filters, each of which has a wavelength dependent transmittance or reflectance, $t_i(\lambda)$. They, together with the solid angle, Ω, subtended by the optical collection system, and the surface area, A_s, of the radiant target, determine the radiant power which reaches the detector,

$$P = \frac{A_s \Omega C_1}{\pi} \int_0^{\infty} \frac{\prod_{i=1}^{n} t_i(\lambda)\, \varepsilon(\lambda,T) d\lambda}{\lambda^5 \left(e^{C_2/\lambda T} - 1\right)} \qquad (2)$$

where n is the number of components in the optical train.

Rather than use Eq. (2), many commercial pyrometers determine the temperature of a surface by comparing the power emitted by it with that of a calibrated source having a known temperature. The temperatures deduced in this fashion are generally referred to as "brightness" temperatures, since they in essence compare, over a broad range of wavelengths, the brightness of the unknown target to the brightness of the calibrated source. Unfortunately, in addition to its dependence on temperature, the radiant emission depends on the emissivity of the hot object, an intrinsic property of the material. As indicated in Eq. (1), the emissivity may be a function of both wavelength and temperature. Due to differences in the emissivity functions of the calibration source and the target material over the range of wavelengths to which the photodetector is sensitive (typically ranging from the near-uv to the near-ir), this reported brightness temperature may differ substantially from the true temperature. In fact, since the wavelength dependence of the emissivity of the target is generally unknown, there is usually little effort made even to estimate the temperature uncertainty with this sort of device.

By using a narrow bandpass optical filter to select a particular wavelength (i.e., color) at which to compare the signal generated by the unknown target to that of the calibration source, a more accurate estimate of the true temperature, called the "color" temperature, can be obtained. This technique has the advantage that the emissivity of the target, and the transmittance or reflectance of other optical components, are essentially constant over the transmitted wavelengths. These variables can therefore be removed from the integral in Eq. (2) and, if the transmission curve of the filter is known, the integral may be evaluated, as

$$P = \varepsilon_\lambda C_\lambda \int_{\lambda_1}^{\lambda_2} \frac{t_f(\lambda) d\lambda}{\lambda^5 \left(e^{C_2/\lambda T} - 1\right)} \qquad (3)$$

where ε_λ is the emissivity at the central wavelength of the filter, C_λ is a constant (independent of temperature) determined by the optical system which may be evaluated by calibration, t_f is the (known) transmission function of the filter, and λ_1, λ_2 are the bandpass limits of the filter. When the photodetectors are operated such that they generate a voltage signal which is proportional to the power incident on their surfaces, Eq. (3) may be written as

$$V(T) = \varepsilon_\lambda B_\lambda F_\lambda(T) \tag{4}$$

where $F_\lambda(T)$ is a known thermal response function proportional to the integral in Eq. (3), and the constant $B_\lambda = GC_\lambda$ where G (Volts/Watt) is the responsivity of the photodetector and its associated amplification circuitry. Reported color temperatures are typically those which correspond to the the voltage signals generated by targets with unit emissivity, i.e., blackbodies. However, if the target's emissivity at the selected wavelength is known, then it is simple to use Eq. (4) to correct the color temperature to the true temperature.

Unfortunately, in most cases of interest the emissivity varies both with temperature and with wavelength, and therefore is difficult if not impossible to evaluate independently. In some instances, the emissivity even changes with time as chemical or structural changes occur in the heated material, as with ceramic materials proposed for manufacture in space which become glassy when heated beyond their melting point, or with many metals which oxidize rapidly when hot. Thus, it is often not feasible to correct the color temperature. A popular scheme for circumventing this problem is to employ a two-color pyrometer, a device which measures the radiant power at two, generally closely spaced, wavelengths. By making an assumption about the ratio of the emissivities at the two wavelengths, the Planck equation can be used to calculate the temperature, as well as the emissivity. Although this technique is useful when the emissivity ratio at the two wavelengths is well-known, its accuracy suffers tremendously by any small errors in that ratio.[2,3]

In contrast, with the appropriate selection of wavelength for a particular range of temperatures, color-temperature measurement with a single pyrometer can be a very accurate measure of the true temperature, being insensitive to a large uncertainty in the emissivity at that wavelength. For values of $\lambda T << 1$, the radiant power emitted by a heated surface increases faster than exponentially with temperature, but is only linearly dependent on emissivity. Thus, a large uncertainty in emissivity causes only a small error in temperature. Mathematically, this is seen by solving the Eq. (4) for temperature. The function $F_\lambda(T)$ may be easily evaluated by approximating the transmission function of the narrow bandpass filter by a rectangle of height t_λ and width $\Delta\lambda = \lambda_2 - \lambda_1$. Then we may define

$$F_\lambda(T) = \left(\exp(C_2/\lambda T) - 1\right)^{-1} \tag{5}$$

and

$$B_\lambda = (A_s \Omega t_\lambda G C_1/\pi)\left(\prod_{i=1}^{n} t_i\right)(\lambda^{-5}\Delta\lambda) \quad . \tag{6}$$

Solving Eqs. (4), (5), and (6) for temperature yields

$$T = (C_2/\lambda)\ \ln^{-1}\left((B_\lambda \varepsilon_\lambda/V) + 1\right) \quad . \tag{7}$$

Differentiating with respect to ε_λ gives the temperature error as

$$\Delta T/T = \left(1-\exp(-C_2/\lambda T)\right)(\lambda T/C_2)(\Delta\varepsilon_\lambda/\varepsilon_\lambda) \tag{8}$$

which is plotted in Figure 1 for a selection of wavelengths using $\Delta\varepsilon_\lambda/\varepsilon_\lambda = \pm 25$ percent. Although the temperature uncertainty increases with temperature for all wavelengths, it is clear that, by selecting a sufficiently short wavelength for operation of the pyrometer, uncertainties below one percent can be achieved.

On the basis of Eqs. (7) and (8), it would appear that a single color pyrometer could be used to measure any temperature below a predetermined value to any degree of accuracy simply by selecting a sufficiently short wavelength.

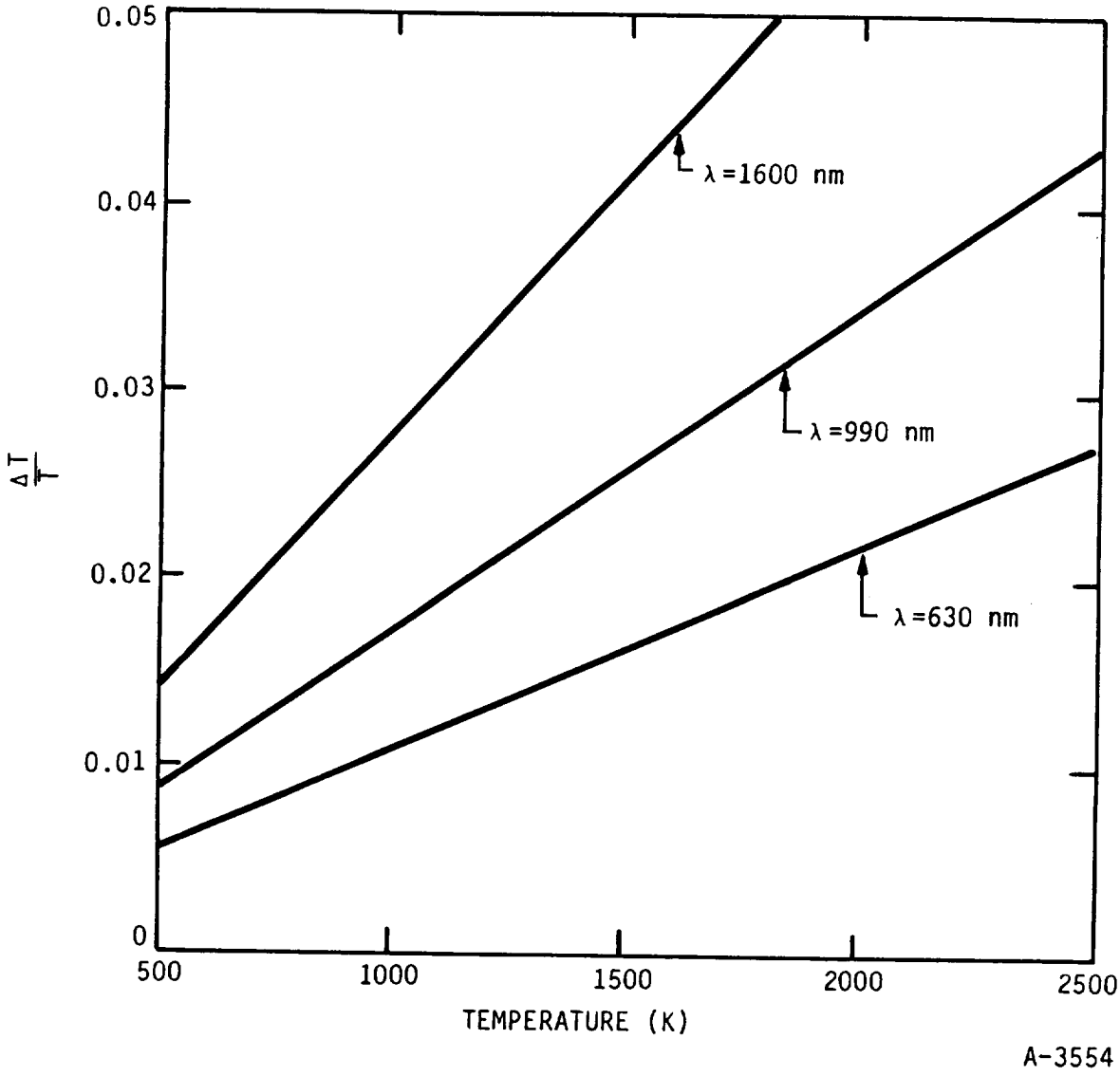

Figure 1. Temperature uncertainty resulting from an emissivity uncertainty of $\Delta\varepsilon/\varepsilon = \pm 0.25$ using a single color pyrometer

Although this is, in principle, true, there is a lower limit on the temperature sensitivity which, for the temperature range of interest, is determined by the noise inherent to the photodetector. In addition, there is a maximum temperature to which a particular optical pyrometer/ photodetector combination will be sensitive, fixed by the onset of detector saturation. A photodetector typically has a dynamic range of about five orders of magnitude. As shown in Figure 2, at a wavelength of 630 nm, where the emissivity related temperature error remains below 2.5 percent up to 2300 K, the radiant power spans well in excess of ten orders of magnitude as the temperature increases from 600 to 2300 K. It is clear that a single pyrometer operating at this wavelength is unsuitable for measurements over the entire temperature range of interest. In contrast, at a longer wavelength (1600 nm for example) the radiant power in this temperature range spans less than seven orders of magnitude. However, as shown in Figure 1, the emissivity related temperture uncertainty becomes excessively large at the higher temperatures. It is clear that, to have both the required range of temperature sensitivity and accuracy of better than ±2.5 percent, a pyrometer operating at multiple wavelengths is required. Examination of Figures 1 and 2 indicates that, using photodetectors which have a five order of magnitude dynamic range, and demanding temperature accuracy of ±2.5 percent, three colors are desirable. Thus, a device utilizing three wavelengths and three photodetectors was designed, as is discussed in the next section.

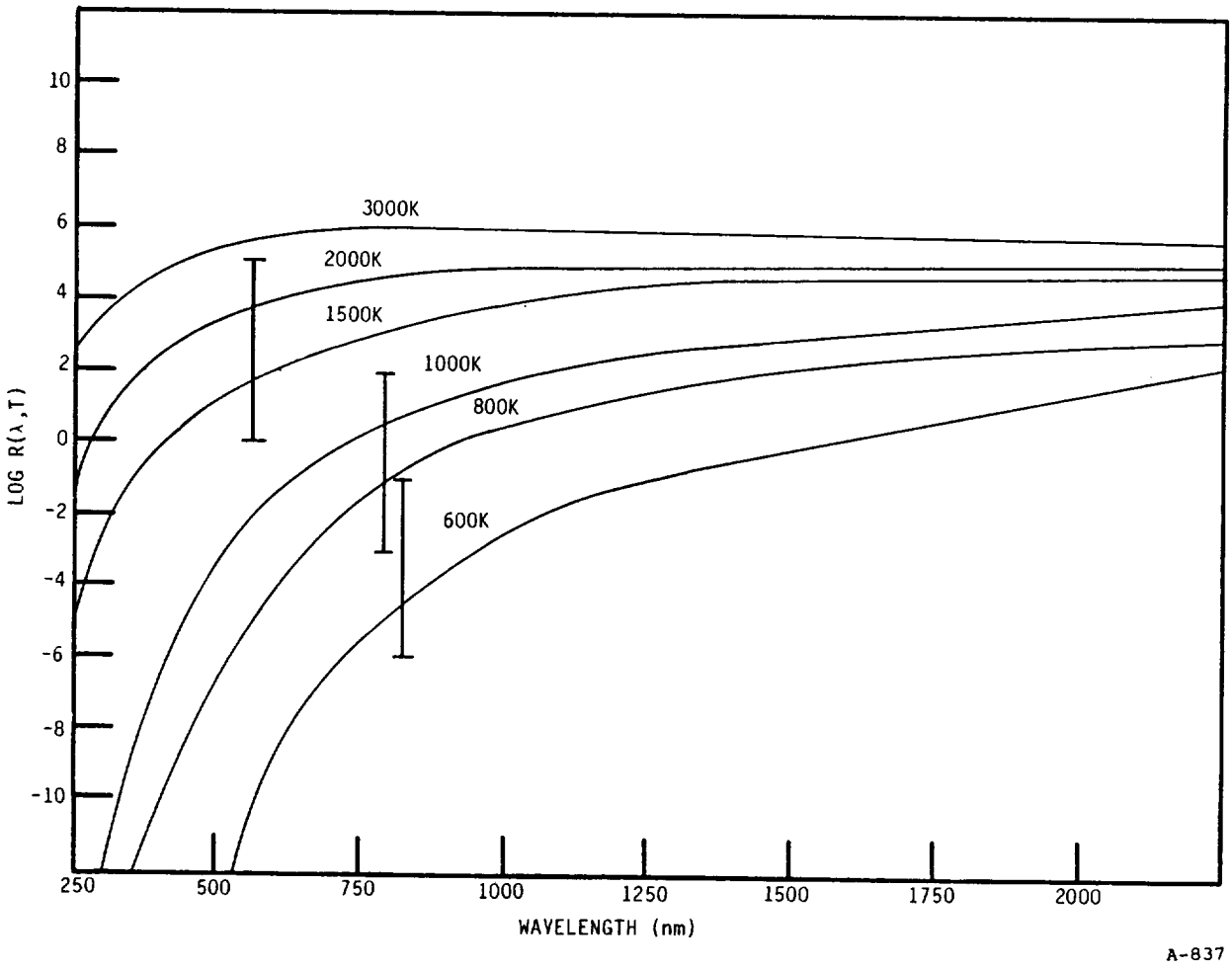

Figure 2. Radiant flux per steradian per unit area of emitter surface per unit wavelength interval emitted from a blackbody

3. PYROMETER DESIGN

3.1 Wavelength Selection

The three wavelengths to be used in the pyrometer were selected on the basis of the following criteria:

1. The device should be sensitive to temperatures ranging from 300 to 2000 C, or 573 to 2273 K.

2. The temperature measurements should be accurate to ±2.5 percent when the emissivity is known only to within ±25 percent of its true value.

3. For maximum precision, each of the three detectors should be sensitive to as small a dynamic range of radiant energies as possible.

The first two criteria specify the shortest of the three wavelengths. Inserting the values T = 2300 K, $\Delta T/T = 0.025$ and $\Delta\varepsilon_\lambda/\varepsilon_\lambda = 0.25$ into Eq. (8) yields a wavelength of $\lambda_3 = 626$ nm. The last criterion is satisfied by designing the pyrometer so that all three detectors cover the same dynamic range, which was found to be about 2.5 orders of magnitude. A surface having a constant emissivity at 626 nm will emit a radiance 2.5 orders of magnitude smaller than that at 2300 K when its temperature is reduced to 1460 K, which, for design purposes, was selected as the maximum temperature to which the mid-range detector is sensitive. Again invoking criterion 2, the optimum wavelength for this middle detector was found to be $\lambda_2 = 987$ nm. Iterating once again, it was found that the minimum temperature for this detector was 926 K. This specified the wavelength of the low-temperature detector as $\lambda_1 = 1556$ nm. At this wavelength, temperatures from 587 to 926 K span 2.5 orders of magnitude in radiance.

The three-color pyrometer was thus designed to use detectors operating at wavelengths around 1600 nm, 990 nm, and 630 nm, with each detector having a linear response over about 2.5 orders of magnitude. For the approximation

used in Eqs. (5) and (6) to be valid, namely that ε and t_i are constants over the bandwidth of each filter, it is essential that the bandwidths be only large enough to allow a detectable level of radiation to pass. For this reason we used three-cavity bandpass filters, supplied by Pomfret Research Optics, which have full-widths of one percent maximum transmission of approximately 20 nm. The precise bandpass filter characteristics are as follows:

Wavelength (nm)	t_λ	Bandwidth (nm)
1600	0.41	12
990	0.69	11
630	0.58	10

3.2 Optical Assembly

Examination of Eq. (2) reveals that, once the bandpass filters have been selected, the amount of radiant power which reaches the photodetector is determined by the solid angle subtended by the optical collection system and the area of the radiant source which is imaged onto the detector. To minimize ease of construction and operation, as well as cost, the electro-optic transducers chosen for construction of a demonstration pyrometer were simple photodiodes combined with operational amplifiers. A germanium photodiode, which is most sensitive to near-infrared radiation, was required for the low temperature detector, while silicon photodiodes were used at the shorter wavelengths. It was assumed that the radiant source would be greater than 1 cm in diameter, and could be positioned within about 10 cm of the pyrometer. Imaging optics were selected which would assure that sufficient radiation reached the detectors to generate a usable signal at the lowest temperatures sensed by each. An assembly structure was designed which allows the three detectors and all associated optics to be fixed in position once and for all time, is lightweight but rigid, and serves as a prototype of a spaceworthy device.

A schematic illustration of the pyrometer's optical layout is shown in Figure 3, and a photograph of the device is presented in Figure 4. A 50 mm

focal length glass condenser lens, comprised of two 100 mm focal length, 38 mm diameter, plano-convex lenses, images the radiant source onto a 1 cm diameter field stop. The radiation which passes through the stop reaches three 50 mm focal length, 25 mm diameter lenses, mounted on a plate in the configuration shown in Figure 5, which re-image the field stop, and thus the 1 cm diameter portion of the source, onto the three photodetectors with 1/3 magnification, resulting in a circular images 3.3 mm in diameter. The solid angle subtended by the optics is 0.012 sr, as limited by the three smaller lenses. The optical elements are all mounted in circular black anodized aluminum plates which are fixed in position with respect to each other by alignment rods passed through key holes in the plates.

The sensitive area of the germanium detector (Judson Infrared Model J16-5SP with a 741 operational amplifier) is a square 3 mm per side. When the image of the source is centered on this detector, an area of 0.080 cm^2 is irradiated. Because the source diameter is three times as large as its image,

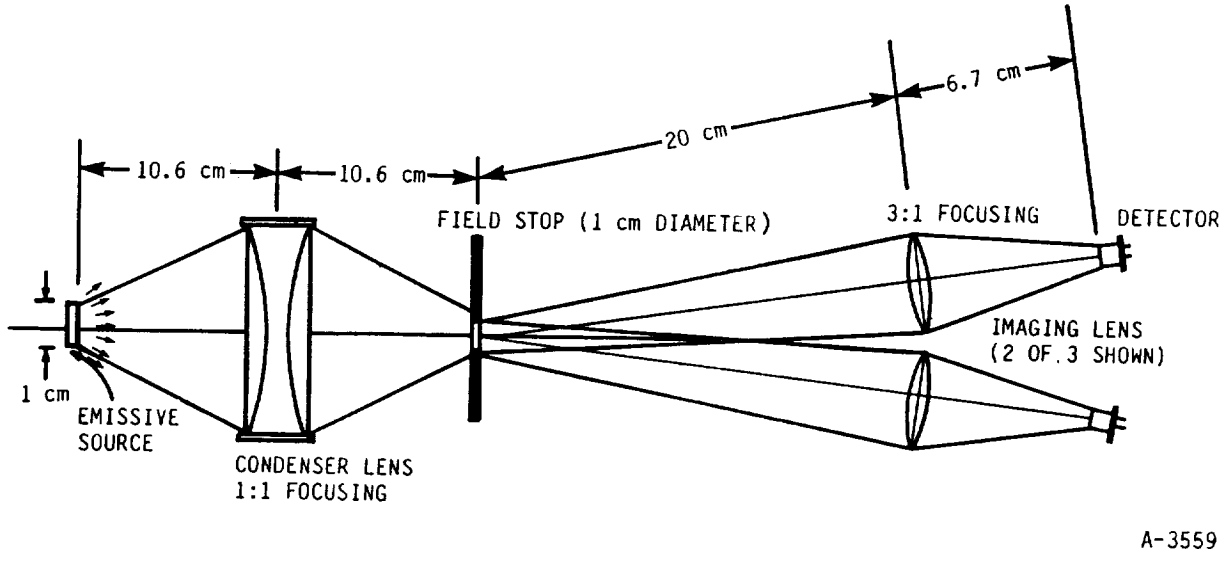

Figure 3. Schematic illustration of multicolor pyrometer optical design

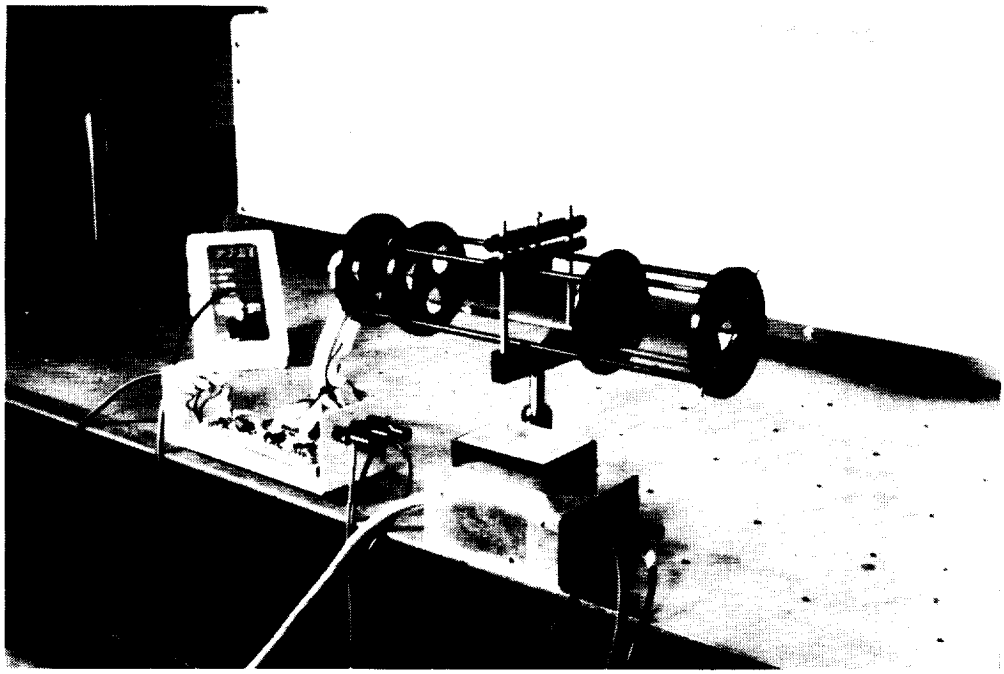

Figure 4. Photograph of pyrometer

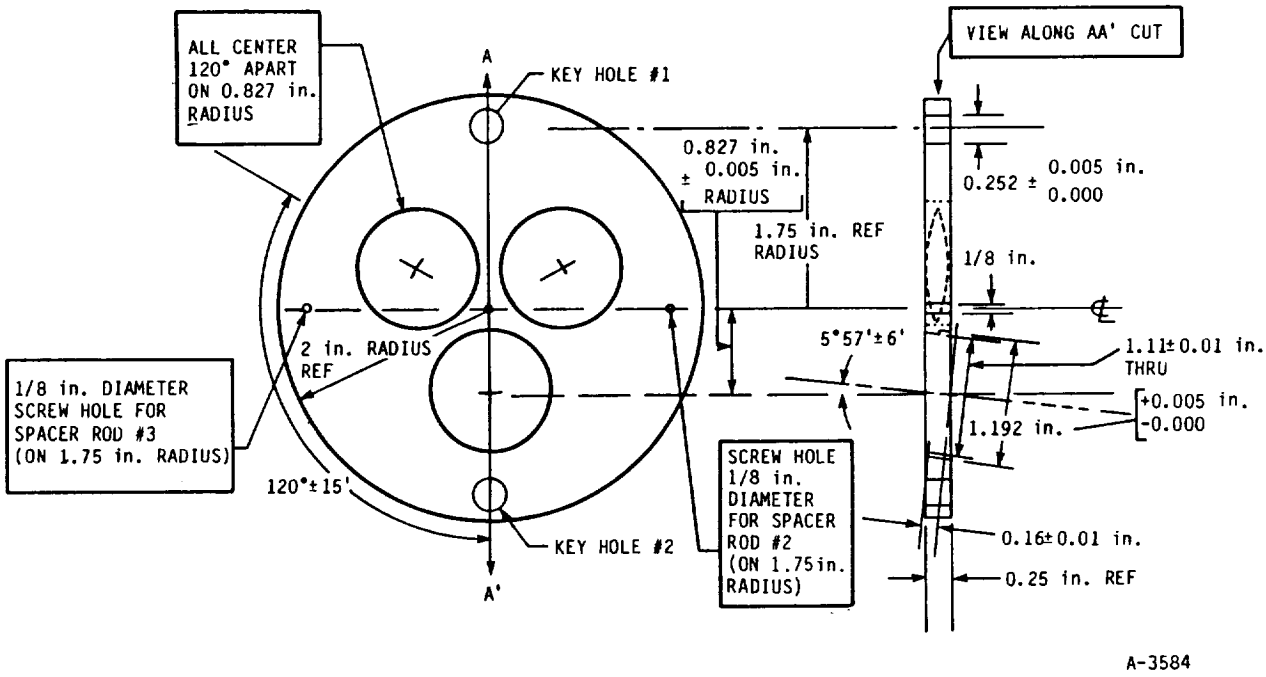

Figure 5. Layout of three imaging lenses

the effective source area is 0.72 cm^2. The two silicon detectors (EG&G Model HAD-1100A photodiode/op-amp combination package) have sensitive areas which are circles 2.54 mm in diameter. When the source image is properly centered on these detectors the entire surface is irradiated. The effective source area is therefore $(9\pi/4)(0.254)^2 = 0.456\ cm^2$.

These numbers can be inserted into Eq. (2) to demonstrate that measurable radiation will reach each detector. An example is presented for the low temperature portion of the pyrometer only. Assuming that: 1) the transmission function of the bandpass filter is a constant equal to t_λ over the wavelength region $[\lambda_1,\lambda_2]$ and zero elsewhere; and 2) the transmission through each of eight glass surfaces (three lenses and the photodetector cover glass) is $t_i = 0.96$, then, for a blackbody source, Eq. (2) can be written as

$$P = (A_s \Omega t_\lambda C_1/\pi)(0.96)^8\ \lambda^{-5}\Delta\lambda\ \left(\exp(C_2/\lambda T) - 1\right)^{-1} \quad .$$

Inserting values for the 1600 nm filter and the germanium detector, and a temperature of 573 K yields a detectable power of 5.2×10^{-9}W. The noise equivalent power (NEP) of this detector with an amplifier bandwidth of 1 kHz is 6.3×10^{-11}W, and the response remains linear until the incident power reaches about 5×10^{-4}W. The incident power thus falls well within the linear regime for all temperatures at which this detector will be used, and the minimum power to which it must be sensitive is well above the noise level. The optical system is therefore well designed for the application. Similar calculations have been performed for the two silicon detectors, yielding similar results.

These numbers can also be used to estimate the calibration constants B_λ (defined in Eqs. (4) and (6)) for each detector. To convert values of incident power to voltages, the responsivity of the detectors (A/W) and the transimpedence (V/A) of the op-amp associated with each detector must be known. The former can be found in the data sheets accompanying the detectors and the latter is simply equal to the resistance of the feedback resistor for each op-amp, which we have selected to be 10^6 for all three detectors. At 1600 nm,

the germanium detector has a responsivity of 0.85 A/W, so G for that detector is 0.85×10^6 V/W, giving an anticipated calibration constant of

$$B_{1600} = 2.9 \times 10^4 V \quad .$$

Similarly, $B_{990} = 1.7 \times 10^5 V$

and $B_{630} = 9.4 \times 10^5 V$

Evaluation of the actual calibration constants is discussed next.

4. CALIBRATION

The calibration constants just calculated are based on the design of the optical system assuming ideal thin lenses, and on idealized transmission functions of the bandpass filters and other optical components. Because the actual lenses have some spherical aberration which reduces the effective solid angle, and the bandpass filter function is not really rectangular, these calculations can only roughly approximate the true calibration constant for each detector. Calibrations were therefore performed using blackbody sources.

A low temperature blackbody, operable at temperatures between 300 and 1273 K, was used to calibrate the two longer wavelength detectors. The source was accurately aligned with the optical axis of the pyrometer by passing a He/Ne laser beam through centering holes in the pyrometer and thence through a 1 mm hole centered on the blackbody's exit aperture. The aperture was then positioned in the source plane of the pyrometer and imaged onto the field stop, thereby also being imaged onto the photodetectors. The aperture diameter was then increased to greater than 1 cm in diameter so that its image filled the field stop, as called for in the pyrometer's design. The temperature of the blackbody was set and allowed to reach a steady value, which was measured by a platinum/platinum-rhodium (13 percent) thermocouple and ice point reference. The voltages produced by the two detectors were measured by a computer-coupled data acquisition system (described in detail later in this report) with a precision of 0.030 mV. They are plotted as functions of temperature in Figure 6. Note that the long wavelength detector is sensitive to temperatures as low as 540 K and greater than 1000 K. The mid-wavelegth detector is sensitive from 750 K to beyond the limit of the blackbody source. Both of these temperature ranges satisfy and even exceed the design goals.

The detector voltages are plotted as functions of $F_\lambda(T)$ in Figure 7a. As expected the relationship between the two parameters is linear over the entire temperature range. The slope of the line is proportional to the calibration constant. After least-squares fitting of the straight lines, the calibration constants are found to be:

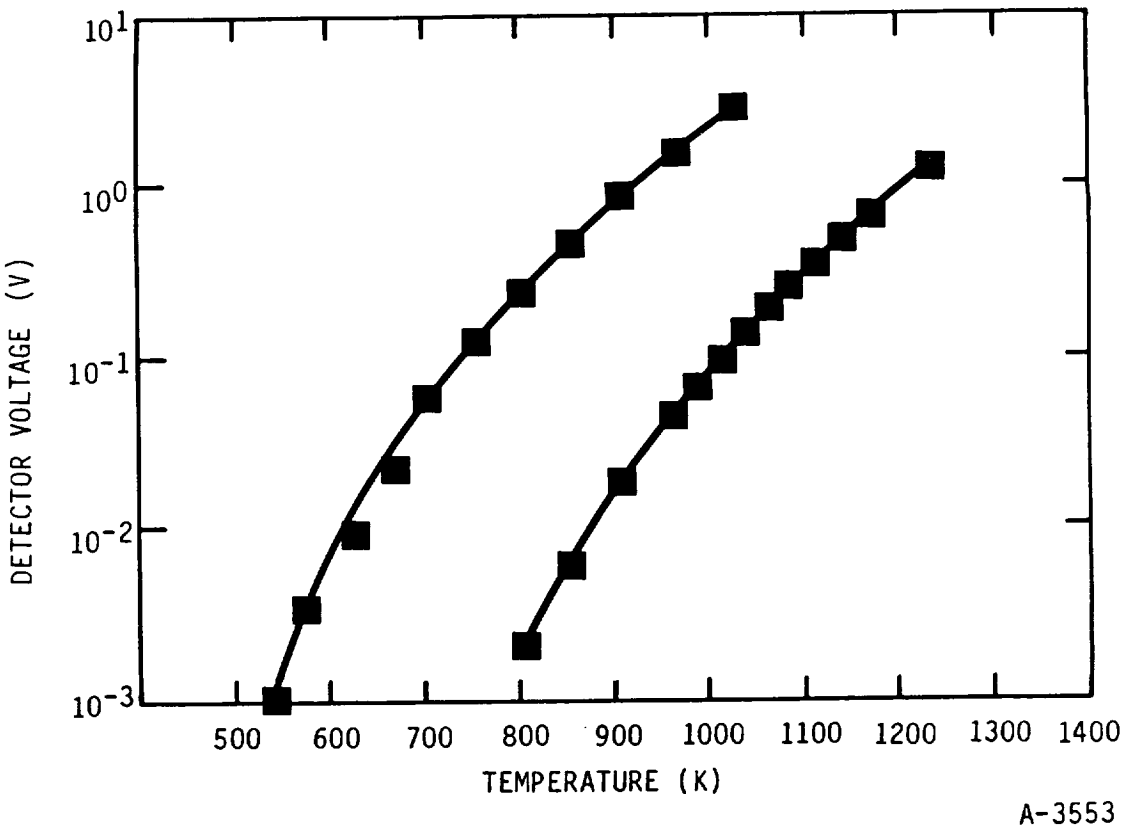

Figure 6. Output voltages versus temperature for the two low-temperature detectors

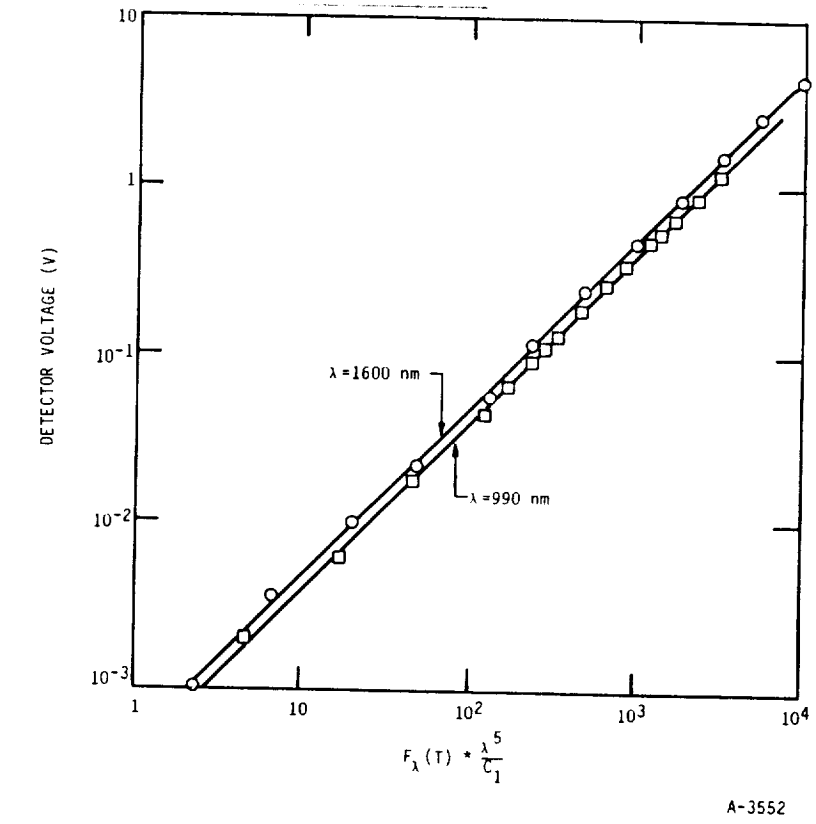

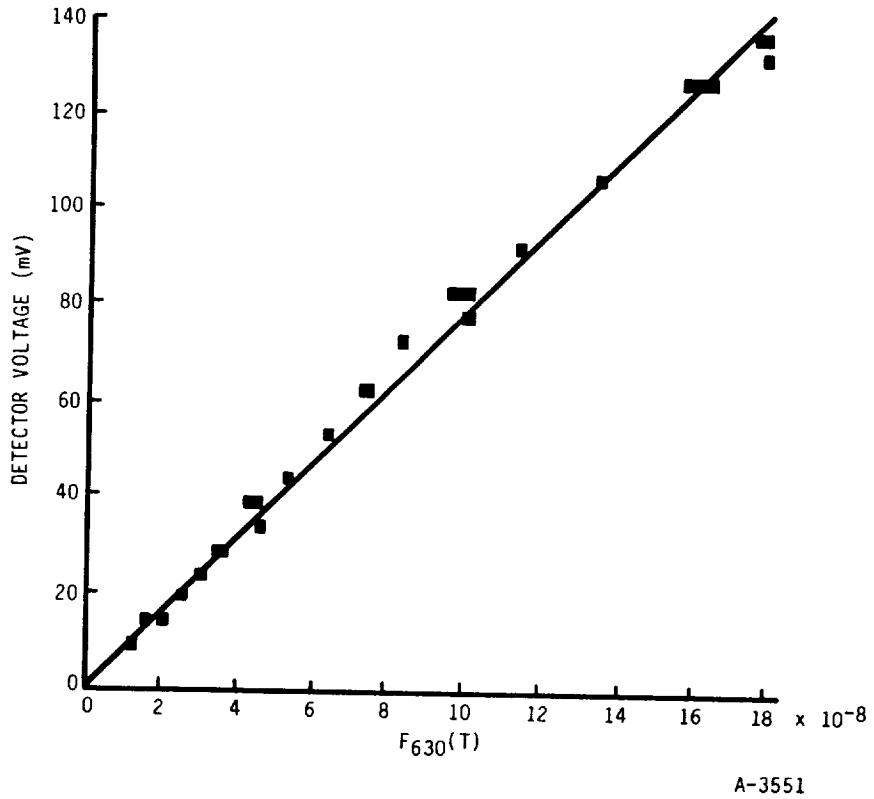

Figure 7. Output voltages versus radiance function for a) the two low-temperature and b) the high temperature detectors

$$B_{1600} = (1.69 \pm 0.01) \times 10^4 \text{ V}$$
$$B_{990} = (1.49 \pm 0.02) \times 10^5 \text{ V} \quad .$$

Because this blackbody source could only achieve a maximum temperature of 1000C, it could not be used to calibrate the short wavelength detector (630 nm). However, we did have available a second blackbody source capable of achieving temperatures in excess of 1800 K. Unfortunately, this source did not have a reliable independent means for ascertaining its temperature. To circumvent this problem we employed a bootstrap procedure. Although the short wavelength detector was designed to measure temperatures only above 1460 K, it was in fact found to be sensitive to temperatures as low as 1250 K. By using the mid-range detector to measure the temperature of this uncalibrated blackbody between 1250 K and 1460 K (above which the mid-range detector rapidly reached saturation) we were able to obtain sufficient data, plotted in Figure 7b, to calculate the high temperature calibration coefficient as

$$B_{630} = (7.81 \pm 0.03) \times 10^5 \text{ V} \quad .$$

All three actual calibration constants are within acceptable limits of their anticipated values. In fact, the calibration constants for both silicon detectors are about 85 percent of their pre-calculated values, while the germanium calibration constant is 55 percent of that anticipated. The larger discrepancy with germanium is probably due to the image of the source not being perfectly centered on the square sensitive area of the detector, resulting in a smaller than expected effective source area. However, since the alignment is mechanically fixed for all time, this calibration constant will remain accurate for any uniformly heated source which is imaged to fill the pyrometer's 1 cm diameter field stop.

5. ACCURACY DEMONSTRATION

To demonstrate the pyrometer's capability to make accurate temperature measurements on objects of unknown (or changing) emissivity, metal plates of copper, aluminum, and stainless steel were heated and observed by the pyrometer while simultaneously measuring their temperatures with an insulated chromel/alumel thermocouple coupled to an electronic ice point reference. The heating in all cases was performed by attaching the metal plates to a ceramic heater, and controlling the power input to the heater with a variable transformer. For the copper and aluminum measurements the thermocouple was inserted into a small hole drilled into the surface of the metal and placed within the pyrometer's field of view, thus assuring that it measured the temperature of the same region as the pyrometer. Good contact between the thermocouple and the metal surface was assured by pressing the metal surrounding the thermocouple junction into the drilled hole.

The 6.3 mm thick aluminum plate was heated to its melting point of 933 K. According to handbook data,[4] the initial emissivity of the aluminum at 1600 nm was less than 0.1, but as the plate heated and oxidized its emissivity increased to approximately 0.4. The copper plate was about 12 mm thick and was heated to approximately 900 K. Upon heating, it quickly oxidized to form a black surface having a fairly high emissivity of about 0.8. The stainless steel, only 1.5 mm thick, was also heated to about 900 K, and oxidized to present a surface having an emissivity intermediate between that of copper and aluminum (0.5 to 0.8). Sufficient time was given before the measurements to allow the oxide coat to cover the surface.

Figures 8a-c show the results of these experiments. In each figure, the temperature as determined by the pyrometer is plotted vs the temperature as measured by the thermocouple. The emissivity which has been assumed to calculate the temperature from the pyrometer data is indicated in each figure, and represents our best guess of the most probable value of the emissivity. Because the metal plates oxidize with time, and their emissivities vary with temperature, these assumed emissivities are certain to be somewhat different

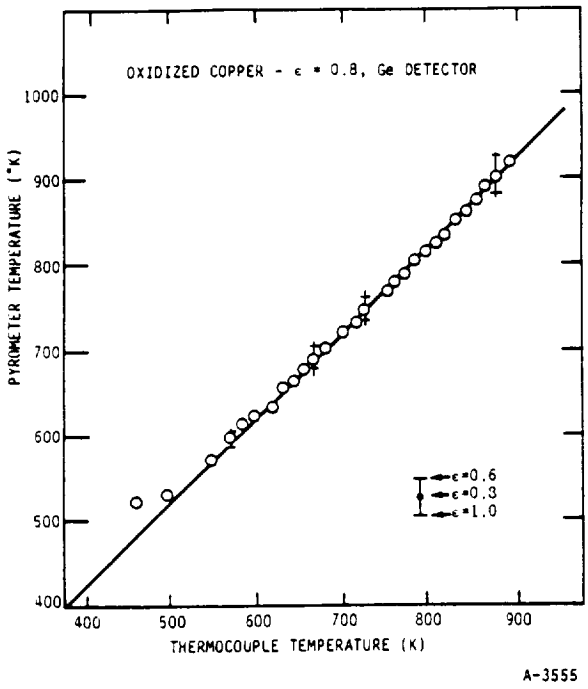

(a)

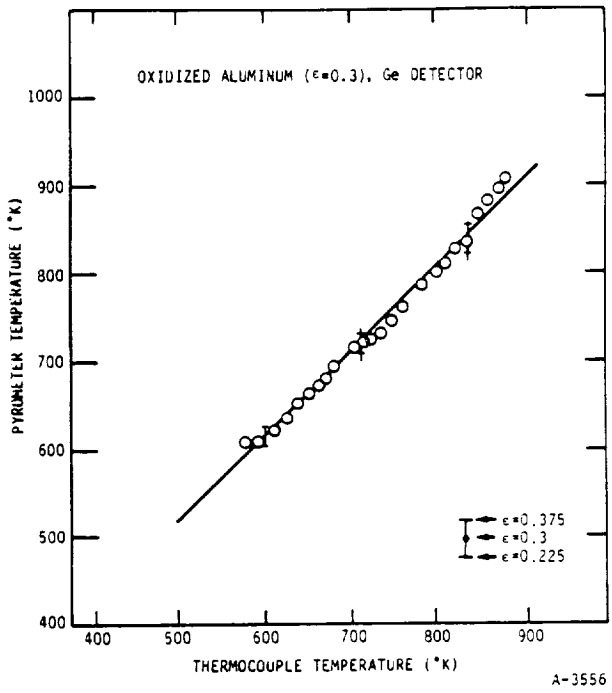

(b)

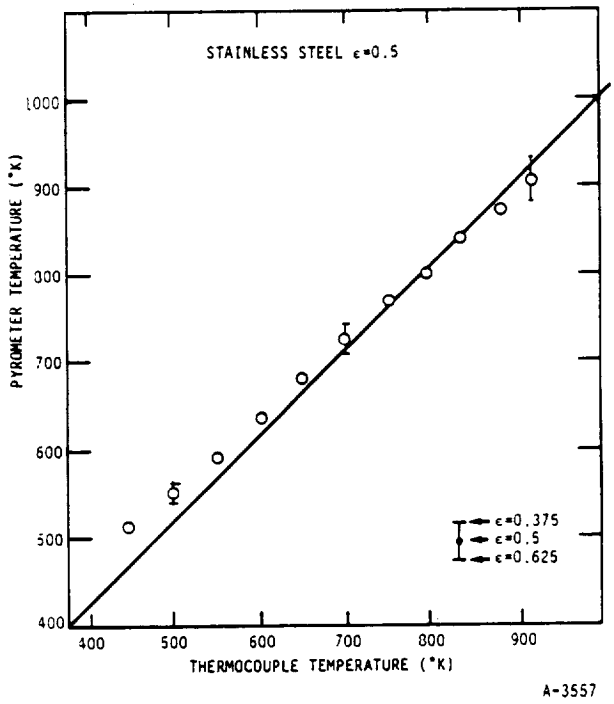

(c)

Figure 8. Comparisons of temperatures measured by pyrometer versus those measured by thermocouple for a variety of heated metal plates

from the actual values. Nevertheless, excellent agreement between the pyrometer and thermocouple measurements is seen in all three experiments, as demonstrated by comparison with the "correct answer" line drawn in each plot as a guide for the eye. Examination of the data shows deviation from perfect agreement of less than one percent at temperatures above 500 K.

Included in these figures are "error bars" for selected temperature points whose endpoints show the temperature which would have been indicated by the pyrometer had an emissivity been assumed that is 25 percent higher and 25 percent lower than that which was actually used. In all cases the error bounded by these two limits is within the 2.5 percent figure predicted.

6. COMPUTERIZED TEMPERATURE CONTROL

For material processing applications, it is desirable to have a capability to not only measure but also control temperatures of heated materials using a non-contact device such as a pyrometer. We therefore chose to demonstrate that our multi-color pyrometer, when coupled with a laboratory computer equipped with a data acquisition and control card, could perform this function. We used a Compaq portable computer as the host for a Data Translation Model DT2801-A data acquisition card. This card simply plugs into one of the slots available for expansion of the computer, and is capable of simultaneously measuring voltages from up to 16 sources with 12 bit (1/4096) precision in the analog-to-digital conversion. It also has provisions for digital output, consisting of two bytes (16 bits) which can be programmed by the user. As described in the following, one of these 16 bits was used as a switch which controlled the power supplied to a heating element, and therefore was able to control the temperature of a heated body.

To use this system as a temperature controller, the three pyrometer voltages were measured by the computer, and a program was written which calculated the temperature corresponding to the voltage in each of the three channels. Obviously, for any given temperature, only one or perhaps two of the channels would give meaningful information. The other channel(s) would either be saturated at their maximum measurable voltage if the temperature was significantly above the maximum temperature for which that detector was designed, or indicate zero if the temperature was well below the design minimum. It was therefore easy to distinguish which channel was calculating the correct temperature, and this capability was built into the data analysis portion of the computer program. The measured temperature was then compared with a preset temperature, supplied by the user to the program, at which the user wanted to stabilize the temperature of a heated body. A subroutine was written which enabled the computer to act as a proportional temperature controller. When the difference between the measured temperature and the preset temperature exceeded a certain value, called the proportional bandwidth, the switch controlling the heating element was held either on or off, depending on whether

the temperature was below or above the preset value. If the switch was on, the body temperature would increase and, conversely, if the switch was off the temperature would decrease. When the temperature reached a point such that it was within the proportional bandwidth of the preset value, the switch was rapidly turned on and off with a duty cycle equal to $0.5(1 - (T_a-T_s)/T_b)$, where T_a is the measured temperature, T_s is the preset temperature, and T_b is the proportional bandwidth. Thus, as the temperature increased towards the preset value, the average power supplied to the heater gradually decreased, and vice versa causing the temperature to ultimately stabilize at a value close to T_s. In general, unless the heating source is grossly over- or under-powered, selection of an appropriate proportional bandwidth and switching speed causes this algorithm to stabilize the temperature of any heated object arbitrarily close to the preset temperature with minimal oscillation.

To test this program, the system was used to control the temperature of the copper block heated as described previously. Now, however, the ceramic heater was connected to an AC outlet through a solid-state relay operated by the output bit of the computer system; no variable transformer was used to control the heater power. From previous experience, it was known that, if the ceramic heater was left on continuously, the copper block would reach a temperature in excess of 900 K. Starting with the copper block at room temperature, a preset temperature of 723 K was entered into the computer and the temperature control program was run, with a proportional bandwidth of 5 K and a switching period of about 10s. A plot of the copper block temperature as a function of time is shown in Figure 9. The temperature rises rapidly, and, with no perceptible oscillation, stabilizes within 1 K of its preset value. Thus, the use of our pyrometer as a non-contact accurate temperature controller has been demonstrated.

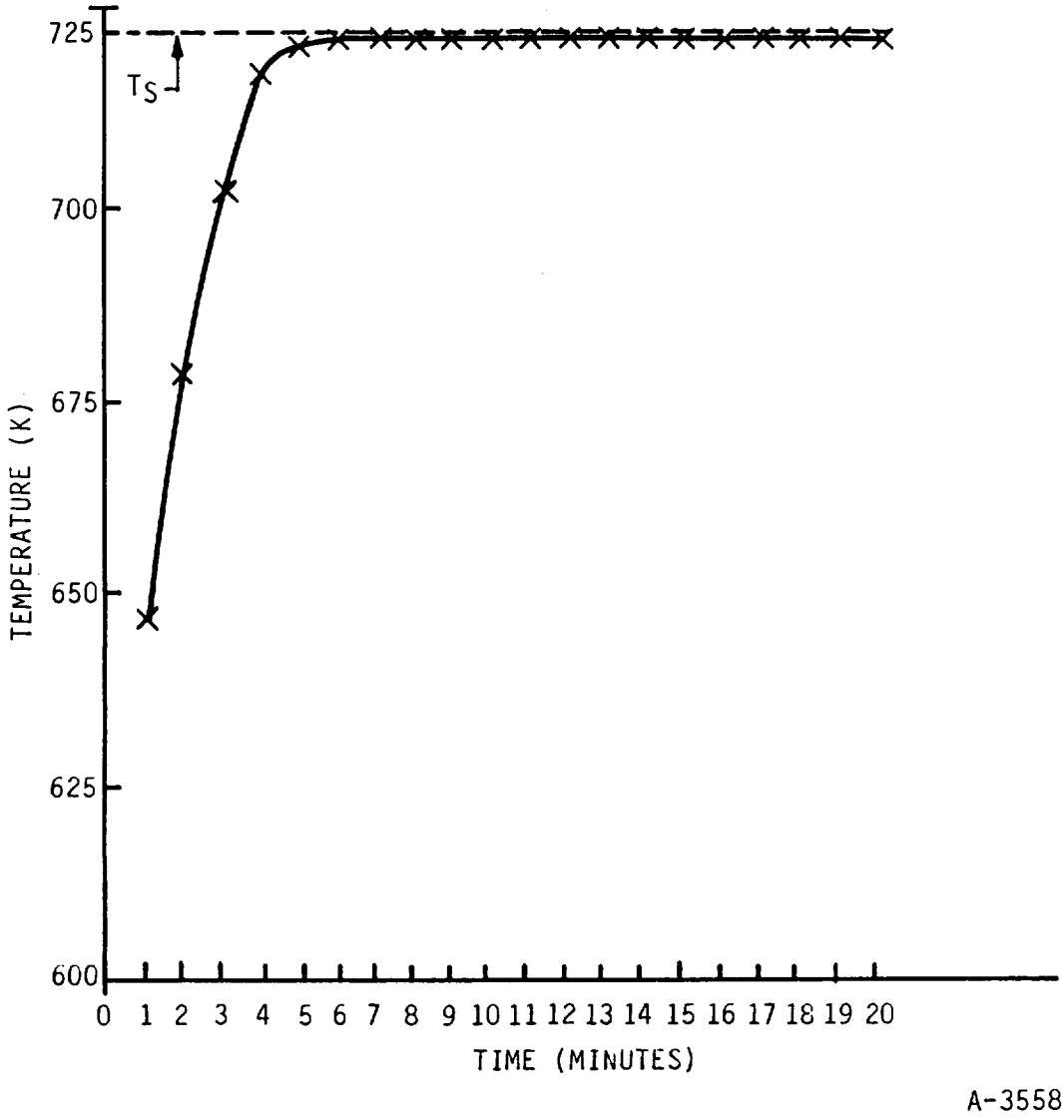

Figure 9. Temperature history of a heated copper plate subjected to the temperature control apparatus

7. SUMMARY

The feasibility of using a multi-color pyrometer to measure and control the temperatures of heated objects, accurately and remotely, has been demonstrated. The pyrometer actually uses only one color at a time, and is relatively insensitive to uncertainties in the heated object's emissivity because the product of the color and the temperature has been selected to be within a regime where the radiant energy emitted from the body increases extremely rapidly with temperature. The device was designed for both simplicity and ruggedness, criteria which are important for an eventual flight instrument, and was constructed with fixed optics in a fashion which makes it easy to align. It was calibrated and shown to exceed its design criteria of temperature measurements between 300 and 2000 C, and its accuracy in the face of imprecise knowledge of the hot object's emissivity was demonstrated. Finally, it was shown that the pyrometer could be easily coupled to a computer and used as a temperature controller.

The demonstration device which has been constructed was designed for use with a hot source located 10 cm away and having a uniform temperature over an area at least 1 cm in diameter. Similar devices can be designed for different geometries. The possibilty exists for designing a pyrometer which incorporates variable focal length optics, although its operation would be more complicated than that described herein. However, by coupling the device to a dedicated computer, programmed with the required data analysis algorithm, the increased complexity could be made transparent to the user. Furthermore, the device can be made completely self-contained and portable by incorporating an appropriately configured and programmed microprocessor in place of the personal computer. We expect to address these possibilities in future work.

ACKNOWLEDGEMENT

The authors thank Larry Piper for his technical review of this work. This project was supported by the NASA Jet Propulsion Laboratory, through Phase I of a Small Business Innovative Research (SBIR) contract.

REFERENCES

1. Siegel, R. and Howell, J.R., Thermal Radiation Heat Transfer, McGraw-Hill (1981).

2. Rosen, D., Lucht, R., Hastings, D. and Weyl, G., "Visible Laser Effects," Report No. TR-268, Physical Sciences Inc., Andover MA (1983).

3. Nordine, P.C., "The Accuracy of Multicolor Optical Pyrometry," High Temperature Science, 21, (1986).

4. Multiple Authors, Handbook of Chemistry and Physics, CRC Press (1985).